MgO addimer diffusion on MgO(100): A comparison of *ab initio* and empirical models

Graeme Henkelman,[1,*] Blas P. Uberuaga,[2] Duncan J. Harris,[3] John H. Harding,[4] and Neil L. Allan[5]
[1]*Department of Chemistry and Biochemistry, The University of Texas at Austin, Austin, Texas 78712-0165, USA*
[2]*Material Science and Technology Division, Los Alamos National Laboratory, Los Alamos, New Mexico 87545, USA*
[3]*Department of Physics and Astronomy, University College London, Gower St., London WC1E 6BT, United Kingdom*
[4]*Department of Engineering Materials, University of Sheffield, Mappin Street, Sheffield S1 3JD, United Kingdom*
[5]*School of Chemistry, University of Bristol, Cantocks Close BS8 1 TS, United Kingdom*
(Received 21 May 2005; published 28 September 2005)

Diffusion of a MgO dimer on a MgO(100) surface is investigated using both density functional theory (DFT) and empirical ionic potentials. Barriers for diffusion via hop and exchange mechanisms are calculated. A qualitative difference is found between DFT and the empirical potential for the oxide exchange barrier. DFT predicts a saddle point for the process with a barrier of 0.88 eV, whereas the empirical potential of Lewis and Catlow, with a formal charge of $\pm 2.0e$, finds this structure to be a stable intermediate minimum with an energy of 0.19 eV, relative to the most stable addimer structure. The empirical potential predicts that the oxide hop and exchange mechanisms are equally likely; whereas, DFT shows that the oxide adion hop mechanism has a lower energy barrier. A Bader population analysis of the DFT charge density indicates that the magnesium and oxide ions have partial charges of magnitude $\pm 1.7e$. Using an empirical potential with this partial charge, the local minimum in the oxygen exchange process becomes a saddle at 0.62 eV, which is in better agreement with DFT. The standard deviation between the energy of the DFT minima and the saddle points with those of the empirical potential was reduced from 0.32 eV when using the formal charge parameters of Lewis and Catlow to 0.15 eV using partial charges. The qualitative agreement found for each diffusion barrier using the partial charge model suggests that a Bader analysis can be used to obtain suitable partial charges for constructing empirical potentials.

DOI: 10.1103/PhysRevB.72.115437 PACS number(s): 68.35.Fx, 68.43.Jk, 31.15.Ar

I. INTRODUCTION

An accurate description of atomic scale mechanisms is critical for predicting collective phenomena such as surface roughness. While density functional theory (DFT) calculations typically afford the accuracy necessary for quantitative prediction, the computational cost is so great that an exhaustive examination of all important mechanisms is often out of reach. Alternatively, empirical potentials overcome this computational cost, but at the expense of chemical accuracy.

Here, we compare predictions for addimer diffusion on MgO(100) using both DFT and Buckingham potentials. We find that a combination of mechanisms typically dominates the system dynamics: a hop or exchange of either the oxide or magnesium ion in the addimer. The details of which mechanism dominates the net mobility of the addimer depend on the description of the system. Full formal charge models of MgO give a qualitatively different diffusion landscape than does DFT. However, a partial charge model, using charges for magnesium and oxygen that are consistent with DFT calculations, results in a landscape that is in better agreement with DFT.

Most measurements of oxide diffusion have been performed on bulk material. Details can be found in the review of Atkinson.[1] Some experiments on MgO grown by molecular beam epitaxy,[2] which are believed to be free of the impurities that dominate all other measurements, support the high values for the Schottky defect creation energy found both in *ab initio* and empirical calculations.[3] Two measurements of surface diffusion[4,5] give inconsistent results, but clearly involve surface vacancies rather than molecules diffusing over the surface. Two previous calculations have been performed on MgO molecules diffusing over an MgO surface. The work of Kubo *et al.*[6] used a quantum calculation to obtain an empirical potential. In this case, Mulliken charges were used to obtain the electrostatic term. An activation energy of 0.25 eV for MgO diffusion was obtained, but the details of the mechanism were not discussed. Geneste *et al.*[7] performed DFT calculations on a number of configurations and predicted that MgO molecules move over the surface, pivoting alternately on the oxide and magnesium ions. The activation energies for these steps are 0.35 eV and 0.46 eV, respectively. Neither paper discusses an exchange mechanism. Exchange mechanisms on metals allow adatoms to diffuse while maintaining a high coordination number throughout the process. In ionic systems, exchange mechanisms also permit diffusion to take place without large changes in the Madelung energy, since one ion enters a given site as the other leaves it. There is the further complication that the electrostatic terms will couple cations and anions; if one species is exchanging with a surface ion, the complementary one will be close by. In this paper, we investigate the diffusion mechanism of the MgO dimer on the MgO(100) surface with both DFT and empirical ionic pair potentials as described by Lewis and Catlow (L-C).[8]

II. RESULTS

A. Density functional theory calculations

Density functional theory calculations were carried out with the VASP[9–12] code, using the Perdew-Wang '91[13]

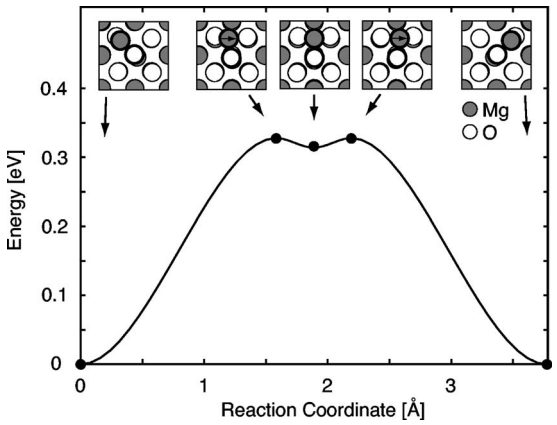

FIG. 1. The magnesium hop process in which a magnesium adion hops from on top of a substrate oxide ion, across a hollow site, onto an adjacent oxide ion site. There is a shallow intermediate minimum of only 14 meV below the saddle energy of 0.33 eV with the magnesium adion at the hollow site. In the final state, the addimer has rotated by 90° about the oxide adion.

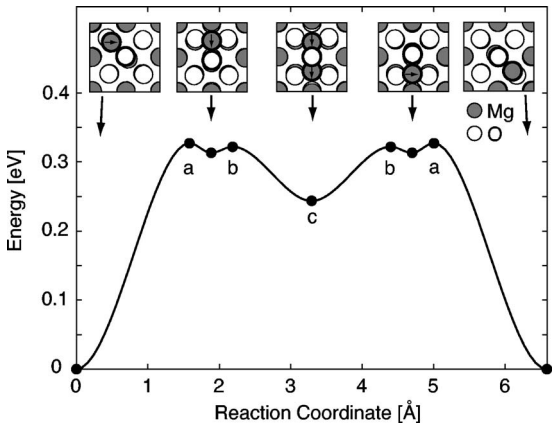

FIG. 2. The magnesium exchange starts in the same way as the hop process, with a magnesium ion moving to an intermediate minimum on a hollow site. From this shallow minimum, the magnesium adion pushes out the surface magnesium ion from directly below the oxide adion into a hollow site. A second half hop moves the magnesium adion to an oxide site. In the final state, the addimer has rotated 180° about the oxide adion, and the magnesium adion has been exchanged with one from the surface.

generalized-gradient approximation (GGA) density functional. A plane wave basis set with an energy cutoff of 250 eV, appropriate for the projector-augmented wave (PAW) pseudo-potentials,[11,14] was used. MgO slabs were modeled with four layers. The addition of a fifth layer does not significantly change the energies of the barriers investigated. A gamma point sampling of the Brillouin zone was found to be sufficient for all but the smallest system size (nine magnesium and oxygen atoms per layer), for which a $2\times2\times1$ Monkhorst-Pack k-point mesh[15] was used.

Energy barriers were found both with the nudged elastic band (NEB)[16,17] method and the minimum mode (min-mode) following method, using a dimer approach to find the lowest curvature mode.[18] The NEB method was used to find the minimum energy path between known minima. Between five and nine images were used to resolve diffusion pathways. The min-mode following method was used to reconverge all saddle points for larger systems with more substrate atoms (where the NEB method, with many images, is more expensive).

B. Magnesium adion diffusion

Two types of diffusion mechanisms were considered for both the magnesium and oxide ions in the surface addimer. The hop process involves one of the ions in the dimer moving to an adjacent site on the surface. The magnesium hop process is shown in Fig. 1. In the initial state, shown in the first inset, the addimer is adsorbed on the surface with the magnesium and oxide ions above their counter ions on the surface. The oxide and magnesium counter ions lift out of the surface by 0.4 Å and 0.5 Å, respectively, to reduce the bond lengths to the addimer. The Mg—O bond length for the addimer is 1.79 Å, which is significantly shorter than the bulk bond distance of 2.12 Å. In the hop process, the magnesium ion crosses a hollow site and moves to the final state, in which the addimer has rotated 90° about the oxide adion. The magnesium hop process has an energy barrier of 0.33 eV. There is a shallow intermediate minimum halfway along the reaction coordinate, in which the magnesium ion rests at the hollow site. The energy of this state is 0.31 eV, only 14 meV below the energy of the saddle. The Mg—O bond distance in the addimer remains relatively constant during the hop processes, increasing only slightly to 1.80 Å at the hollow site minimum. The saddle point geometries along the hop process are very close to the intermediate minimum. The magnesium ion is displaced by only 0.25 Å toward the oxide sites at the saddles.

The magnesium exchange mechanism is illustrated in Fig. 2. The first part of the exchange process (a) is the same as the hop—the magnesium ion moves to a hollow site. From the hollow site, the hopping magnesium adion replaces the magnesium ion directly below the oxide adion by pushing it up into a hollow site. The saddle point geometry for this exchange mechanism is very similar to the hollow site minimum. By passing over an additional barrier of 9 meV above the hollow minimum [(b) with overall barrier of 0.32 eV], the magnesium adion can move in a perpendicular direction to the hop motion into another intermediate minimum [(c) with energy of 0.24 eV] in which the oxide adion is supported on top of the two exchanging magnesium ions. In this geometry, which is illustrated in Fig. 3(a), the oxide adion is 2.8 Å above the surface, which is raised 0.3 Å above its position in the addimer. The two supporting magnesium ions are 1.5 Å above the surface, lowered 0.8 Å below the magnesium position in the addimer. From this intermediate magnesium exchange minimum, a symmetric process brings a magnesium ion back to the surface to form the stable addimer.

The magnesium exchange process shown in Fig. 2 is not the only way the magnesium ion can exchange. The hop and exchange processes are connected as shown in Fig. 4. Combinations of magnesium hop and/or exchange events can result in the magnesium adion being in one of four possible

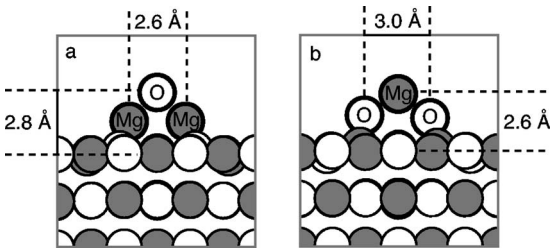

FIG. 3. Intermediate minima along the magnesium and oxide exchange minimum energy pathways. The magnesium exchange minimum (a) is stable with an energy of 0.24 eV, whereas the oxide exchange minimum (b) is unfavorable with an energy of 0.88 eV, just 1 meV below the saddle point energy. The high energy of the oxide exchange intermediate forces the oxide adion to diffuse via the lower energy hop process, whereas the magnesium hop and exchange mechanisms are equally likely.

oxide sites adjacent to the oxide adion. Both processes have to overcome the magnesium hop barrier of 0.33 eV, so they are equally likely to occur. These events alone cannot be responsible for addimer diffusion because the oxide adion does not move. Addimer diffusion will take place only by combinations of oxide and magnesium diffusion events.

C. Oxide adion diffusion

The diffusion mechanisms for the oxide adion are similar to those described for magnesium with the identity of the ionic species switched. The energy landscape, however, is substantially different. The oxide adion hops with a higher barrier of 0.43 eV. No intermediate minimum is found with the oxide adion at a hollow site—instead this geometry is the saddle point for the hop process. The oxide exchange process does have a very shallow intermediate minimum, only

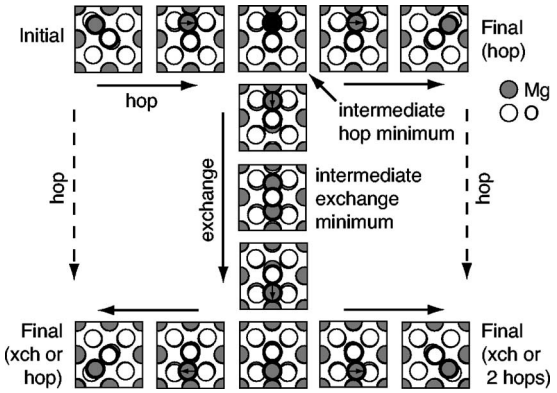

FIG. 4. Connectivity of hop and exchange diffusion processes for the magnesium ion in the MgO addimer as found with DFT. The top and bottom rows illustrate the hop process and an intermediate minimum. These intermediate minima are connected with an exchange process, in which the magnesium adion exchanges with the magnesium ion below the oxide adion. Another intermediate minimum is found along this pathway, in which the oxide ion is supported on the bridge formed by the exchanging magnesium ions. Similar diffusion mechanisms are found for the oxide ion, except in that case there is no intermediate minimum for the hop process.

1 meV below the saddle point energy of 0.88 eV. In the saddle point geometry, the magnesium adion is supported on the bridge formed by the exchanging oxide ions. Figure 3(b) shows this geometry and illustrates that the magnesium adion is able to get closer to the surface due to a larger separation of the supporting oxide adions than the oxide adion can in the magnesium exchange process [see Fig. 3(a)]. In both cases, the supported adion is 0.3 Å higher than its position in the initial addimer configuration.

The most significant difference between the geometries in Fig. 3 is the energy. Figure 3(a) is a fairly stable intermediate minimum along the magnesium exchange pathway with an energy of 0.24 eV, whereas Fig. 3(b) is a very shallow minimum (almost a saddle point) along the oxide exchange pathway with an energy of 0.88 eV. One reason that oxide exchange is unfavorable compared to magnesium exchange is that the oxide ion is much larger. Size will tend to make the exchange unfavorable as the ions need to push by each other. Size is not a significant factor for the hopping mechanism on the surface, where the barriers for the two species are similar.

A picture of MgO addimer diffusion emerges from these calculations. The saddle point energy for magnesium diffusion is similar for the hop (0.33 eV) and the exchange (0.32 eV), and the overall barrier is the same since a hop to the hollow site is required for the exchange process. This barrier is 0.1 eV lower than the oxide diffusion barrier, so magnesium diffusion will not limit addimer diffusion. The oxide hop process has a barrier of 0.43 eV, which is substantially lower than the oxide exchange barrier of 0.88 eV. Thus, DFT predicts that the magnesium adion will diffuse rapidly around the oxide adion, which in turn will hop along the surface. The overall addimer diffusion barrier is 0.43 eV.

D. Convergence with system size

The energy barrier for the hop and exchange processes for both the magnesium and oxide ions were found as a function of system size. Figure 5 shows the barrier for each process on substrates ranging from 3×3 to 6×6 MgO units in the surface plane, each with four layers. These substrates, shown as inset figures, contain between 18 and 72 ions per layer. The hop processes converge quickly with system size because there is little surface relaxation along the minimum energy path. The exchange processes, in contrast, have a relaxation of about 5% in the barrier in the largest cell (72 ions per layer), compared to the next largest cell (50 ions per layer). Decaying exponential functions, fitted to a plot of the exchange barriers as a function of system size, indicate that the barriers for diffusion on the largest slab overestimate fully converged barriers by 3–4%.

E. Empirical potential calculations

Although density functional theory can be used to find accurate diffusion pathways, it is too expensive for exhaustive exploration of the energy landscape for all but the simplest systems. In order to study diffusion and growth on realistic oxide surfaces, an empirical potential must be found. The physics of ionic systems can be modeled fairly accurately with a pairwise Coulomb interaction between

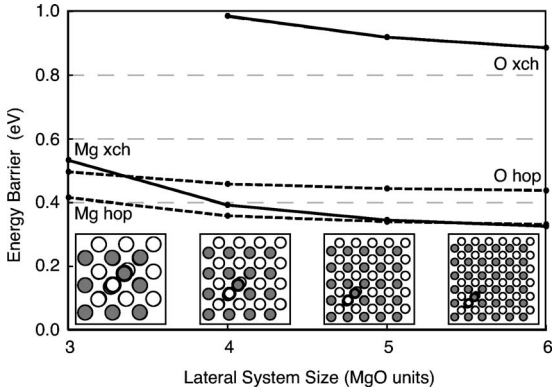

FIG. 5. Convergence of MgO diffusion barriers via both hop (dashed) and exchange (solid) mechanisms. The localized hop processes converge rapidly with system size, overestimating the converged barrier by only 0.03 eV with a substrate of 4×4 MgO units per layer. The exchange (xch) mechanisms converge slowly with system size due to the relaxation of surrounding substrate ions. Fitting an exponentially decaying function to the exchange barriers as a function of number of MgO units in the simulation cell indicates that the barriers of 0.88 and 0.32 eV for the oxide and magnesium exchange, respectively, overestimate the converged barriers by 3–4%.

point charges, a short-range repulsion (arising from to the Pauli exclusion principle), and a weak van der Waals interaction. A pairwise potential of this (Buckingham) form,

$$V_{ij}(r_{ij}) = \frac{q_i q_j}{r_{ij}} + A_{ij}\exp(-r_{ij}/\rho_{ij}) - \frac{C_{ij}}{r_{ij}^6}, \qquad (1)$$

using an exponential function for the repulsive term has been fitted for MgO by Lewis and Catlow.[8] (One should note, incidentally, that DFT methods do not contain the physics of the van der Waals term for well-separated atoms). The parameters of their fit, which assumes formal charges of $\pm2e$ on the magnesium and oxide ions, respectively, are given in Table I (L-C $\pm2.0e$). Cations interact with other cations only through the Coulomb interaction.

It should be noted that the Lewis and Catlow parametrization includes a shell model.[19] This couples the ionic polarization to the short-range forces between the ions. Each ion is modeled as a massive core linked to a massless shell by a harmonic spring constant. Short-range forces act only between the shells, but electrostatic forces act between all cores and shells unless the core and shell is on the same ion. The use of shells greatly increases the computational effort, so for molecular dynamics calculations they are often omitted (producing the rigid ion model). All the calculations discussed below are rigid ion calculations unless otherwise stated.

TABLE I. Parameters for the empirical (Buckingham) potential as fitted by Lewis and Catlow (L-C $\pm2.0e$) and Ball and Grimes using both formal (B-G $\pm2.0e$) and partial charges (B-G $\pm1.7e$) on the ions.

		Parameter		
Model	Interaction	A (eV)	ρ (Å)	C (eV Å^6)
L-C $\pm2.0e$	Mg^{2+}—O^{2-}	821.6	0.3242	0.0
	O^{2-}—O^{2-}	22 764.0	0.1490	27.88
B-G $\pm2.0e$	Mg^{2+}—O^{2-}	1279.69	0.299 69	0.0
	O^{2-}—O^{2-}	9547.96	0.219 16	32.0
B-G $\pm1.7e$	$Mg^{1.7+}$—$O^{1.7-}$	929.69	0.299 09	0.0
	$O^{1.7-}$—$O^{1.7-}$	4870.0	0.2670	77.0

Studies of radiation damage in bulk MgO, using the Lewis and Catlow potential, have shown that multiatom concerted mechanisms are important for annealing.[20] It was also found that diffusion barriers calculated with this potential were consistent with DFT calculations. Similar agreement for surface diffusion barriers would suggest that standard ionic potentials could be used to model dynamics at surfaces as well. In order to test this hypothesis, we calculated the hop and exchange barriers with the Lewis and Catlow potential to see how they compare with our DFT calculations.

Surface diffusion barriers were found using a similar combination of saddle point finding methods as before. In addition, the temperature accelerated dynamics (TAD)[22,21] method was used both to investigate available diffusion mechanisms and to simulate addimer diffusion directly.

The magnesium and oxide diffusion barriers for the exchange and hop mechanisms are listed in Table II. The oxide hop barrier of 0.40 eV is similar to the DFT result, but an intermediate minimum at 0.28 eV is found, which is not observed in the DFT calculations. The Mg hop and exchange barriers are overestimated by about 0.15 eV. Trial calculations using the full-shell model of Lewis and Catlow[8] show only small differences from the rigid ion results reported in detail here. For example, the difference in the saddle point energies (column sp in Table II) for both Mg and O exchange mechanisms between rigid ion and shell models is less than 0.01 eV.

The energy of the oxide exchange processes is qualitatively different. Whereas DFT predicts a high barrier of 0.88 eV and a shallow intermediate minimum with a similar energy, the Lewis and Catlow parametrization predicts a much lower barrier of 0.40 eV and a low energy intermediate minimum of 0.19 eV. The 0.7 eV difference in the energy of this intermediate structure indicates that the Lewis and Catlow parameters cannot reproduce the DFT energy landscape of surface diffusion.

F. Bader charges

The discrepancy of ~0.7 eV between DFT and the (L-C $\pm2.0e$) potential for the oxide exchange barrier leads us to consider how the potential parameters could be determined from DFT. One parameter that can be estimated directly from the charge density is the charge on the ions in the MgO slab. Bader proposed an *atom in molecules* (AIM) approach for partitioning the charge into a set of regions associated with each atom.[23] A strength of Bader's approach is that it depends only on the charge density and not the orbitals used. This makes the method appropriate for use with systems in which delocalized plane waves are used as a basis set. The

TABLE II. The energies of saddle points (sp) and intermediate minima (min) structures for the hop and exchange (xch) mechanisms of the magnesium and oxide ions in the MgO dimer on MgO(100). Energy values are reported in units of eV with respect to the lowest energy MgO dimer structure. Various models are compared, including density functional theory (DFT), the empirical potentials of Lewis and Catlow (L-C) with formal ±2.0*e* charges, and of Ball and Grimes (B-G) with both ±2.0*e* and partial ±1.7*e* charges. The energy barrier for each process is the energy of the sp. If an intermediate minimum was found, its energy is recorded in the min column; a dash is used to indicate that no such minimum was found.

	O hop		Mg hop		O xch		Mg xch	
Model	sp	min	sp	min	sp	min	sp	min
DFT	0.43	—	0.33	0.31	0.88	0.88	0.32	0.24
L-C ±2.0*e*	0.40	0.28	0.48	0.39	0.40	0.19	0.48	0.36
B-G ±2.0*e*	0.52	—	0.51	—	0.52	0.37	0.51	0.32
B-G ±1.7*e*	0.55	0.55	0.37	—	0.62	—	0.37	0.24

AIM approach divides the charge density by surfaces defined by the condition that the charge density along the direction of the surface normal is at a minimum at the surface. The total charge inside these so-called zero-flux surfaces is associated with the ion inside the surface. We have used a recently developed implementation of Bader's method which is fast, robust, and appropriate for plane-wave DFT calculations of solids.[24]

The results of a Bader analysis of the MgO addimer adsorbed on a slab of 200 atoms is shown in Fig. 6. We find an average charge transfer between magnesium and oxygen ions of 1.73*e*, which is consistent with what has been found previously in bulk MgO,[25] and the value of 1.72*e*, found using a different Bader analysis algorithm implemented in the ABINIT package.[26] Deviations from this average charge transfer are seen only in the immediate vicinity of the addimer (see Fig. 6 inset). A smaller charge of −1.56*e* is found on the oxide adion and 1.54*e* is found on the magnesium adion. Although charge transfer from adsorbed species could be important for surface diffusion, we have focused on the primary difference between the bulk charge values as predicted by DFT and the formal charges used in standard empirical potentials. To investigate this effect, we have tested an empirical potential with partial ionic charges of ±1.7*e*, roughly matching the Bader charges from DFT.

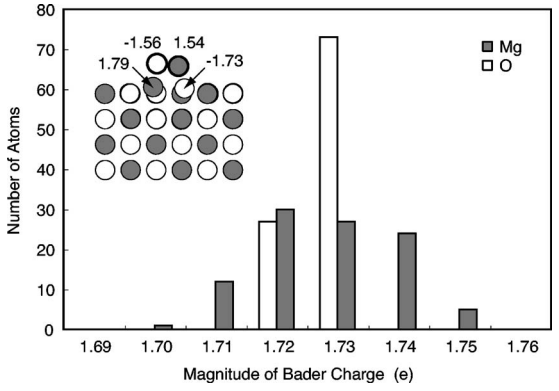

FIG. 6. Histogram of the magnitude of Bader charges for ions within a 200 atom slab with an adsorbed MgO dimer on the surface. Magnesium ions have a positive charge and oxide ions have a negative charge. The distribution of charge transferred from magnesium to oxide ions is peaked about the average value of 1.73*e*. The charge of the atoms in the adsorbed dimer and the nearest surface oxygen atom fall outside the range of the plot. The charge on these atoms is indicated in the inset cross section of the slab.

Recently, empirical potentials were fitted for MgO by Ball and Grimes (B-G), using both formal and partial charges.[27] The oxygen-oxygen interaction is based upon periodic Hartree-Fock calculations of Gale *et al.*[28] for Al_2O_3. Unless the interionic distances are very short, the effect of the differences between this potential and that of Lewis and Catlow is small. At short interionic distances, the strongly repulsive term in Ref. 27 becomes significant as shown below. Each diffusion mechanism investigated with DFT was also studied using their formal (B-G ±2.0*e*) and partial (B-G ±1.7*e*) charge parameters (see Table I). Calculated diffusion energy barriers and intermediate minima are listed in Table II. Particular attention was paid to the oxygen exchange mechanism, for which a qualitative difference of 0.7 eV was found between DFT and the Lewis and Catlow potential (L-C ±2.0*e*). Figure 7 shows the minimum energy path of oxygen exchange for each model. The two potentials based on formal charges show the similar trend of a low diffusion barrier and a low energy intermediate minimum. The difference between the two is related to the choice of the O—O interaction parameters. The partial charge model (B-G ±1.7*e*), in contrast, does not have an intermediate minimum, and the barrier is raised to 0.62 eV, in much closer agreement with DFT. Furthermore, the average energy deviation between DFT and the empirical results of stationary points along the diffusion mechanisms tested is significantly lower for the partial charge model. The formal charge models have a standard deviation of 0.32 eV and 0.27 eV for the L-C ±2.0*e* and B-G ±2.0*e* parameters, respectively. The deviation of the B-G ±1.7*e* potential from the DFT result is 0.15 eV almost half that of the formal charge potentials. This is evidence that a partial charge of ±1.7*e* results in a potential for surface diffusion on MgO, which better reflects the DFT potential energy surface than do the formal charge potentials.

G. Temperature accelerated dynamics simulations

In order to understand better how the two empirical potential models (B-G ±2.0*e* and ±1.7*e*) differ in their descrip-

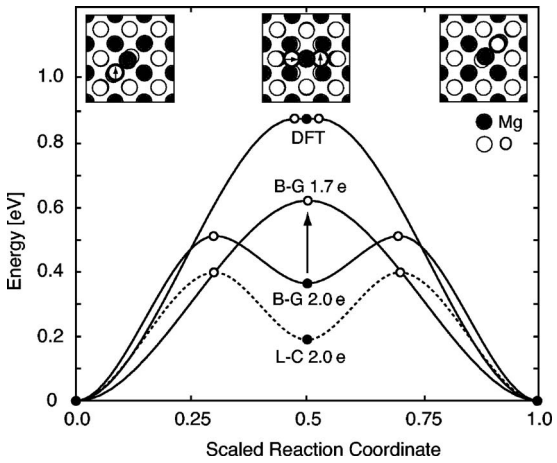

FIG. 7. Energy barriers for the oxygen exchange mechanism. The formal ($\pm 2.0e$) charge models of Lewis and Catlow (L-C) and Ball and Grimes (B-G) predict a low energy intermediate split oxygen structure, in qualitative disagreement with the density functional (DFT) calculations. A reduction in the ionic charge to $\pm 1.7e$ in the Ball and Grimes potential causes the oxygen split structure to become a saddle point at 0.62 eV instead of a minimum at 0.37 eV, bringing the energy 50% closer to the DFT value of 0.88 eV.

tion of addimer diffusion on MgO, we used TAD to explore the long-time behavior of both models. TAD has been described in detail elsewhere.[21,22] Here, we give a brief overview of the method. TAD is one of a number of accelerated dynamics methods which has the goal of simulating system dynamics on times inaccessible to direct molecular dynamics. TAD accomplishes this by using a temperature T_{high} that can be much higher than the temperature of interest T_{low} to explore the dynamics of a given state of the system. However, rather than letting the system move from state-to-state at this high temperature, which would necessarily lead to incorrect dynamics at the low temperature, the system is constrained so that it cannot leave the energy well in which it resides. Instead, when an event is attempted at T_{high}, the event is characterized by finding the energy barrier for that event and the time at which the event occurred is extrapolated to T_{low}. This extrapolation is exact provided the system obeys harmonic transition state theory. The high-temperature exploration of the state is continued until a stopping time is reached, which is defined by two parameters: (i) δ, the uncertainty that we have not accepted the correct event, and (ii) ν_{min}, the assumed minimum prefactor in the system. For our simulations, we have used $T_{high}=1500$ K, $\delta=0.05$, and $\nu_{min}=10^{12}$ s^{-1}. Once this stopping time has been reached, the event with the shortest low-temperature time is selected, the system is moved to that state, and the process is repeated.

We compared the long-time dynamics predicted for the MgO dimer for each of the Ball and Grimes parametrizations. We see both a large qualitative as well as a small quantitative difference in the predicted diffusive behavior. For the B-G $\pm 2.0e$ model, we see that diffusion occurs via a sequence of oxygen and magnesium ion hops and exchanges. In a simulation of 1 μs, a total of 362 transitions were observed. The majority of the transitions were to intermediate

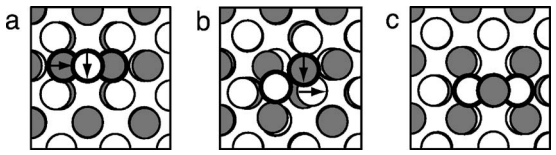

FIG. 8. Diffusion process found during a temperature accelerated dynamics simulation. The intermediate structure (b) between a magnesium exchange intermediate (a) and the oxide exchange intermediate (c) has an energy of 0.35 eV and 0.48 eV with the B-G $\pm 2.0e$ and $\pm 1.7e$ models, respectively. The high energy of the final oxide exchange intermediate minimum makes this process unfavorable according to DFT and the reduced charge B-G $\pm 1.7e$ model.

minima. A total of 80 events led to net magnesium or oxygen diffusion, and these were divided roughly equally between the four possible processes: oxygen hop (18) and exchange (19), magnesium hop (10) and exchange (33). This is expected from the similar energy barrier for each process (between 0.51 and 0.52 eV) and is consistent with a transition state theory rate of 29 transitions per microsecond at 500 K assuming the standard prefactor of 5×10^{12} s^{-1}. Each event takes the system through an intermediate exchange minimum. In addition, we saw one other type of diffusion event, shown in Fig. 8, in which a magnesium exchange intermediate minimum (a) moved to an oxide exchange intermediate minimum (c) via a structure with the magnesium and oxide ions both in hollow sites (b). This structure has an energy of 0.35 eV compared to the addimer.

In contrast, for the B-G $\pm 1.7e$ model, there is a separation in time scales between magnesium and oxide ion diffusion events. Net diffusion for the addimer occurs via oxide hop events as predicted by DFT. In a simulation of 1 μs, we saw nine such events which moved the center of mass of the addimer. For each of these events, there are over 300 magnesium diffusion events, both exchange and hop. We did see two events in which the system visited the structure shown in Fig. 8(b). In both cases, it happened from a magnesium intermediate exchange minimum and returned immediately to the same magnesium intermediate exchange minimum. In this parametrization, it has an energy of 0.48 eV above the addimer.

From these runs, we do not have enough statistics to directly calculate diffusivity for the two models. However, reducing addimer mobility to the occurrence of oxide events, as they are the rarer event in the $\pm 1.7e$ model, we see that diffusivity will be governed by oxide ion hops in the $\pm 1.7e$ model and a combination of oxide ion hops and exchanges in the $\pm 2.0e$ model. This is consistent with the results in Table II. At 500 K, the difference between oxide ion hop rates predicted by the two models is a factor of two, assuming the rate prefactor is the same for both models. Thus, quantitatively, there is little difference in what the two models predict in terms of overall diffusivity.

There is, however, a qualitative difference in how the addimer diffuses between the two models. As the $\pm 1.7e$ model predicts that oxide diffusion occurs only via hops, the identity of the oxide ion in the addimer will remain constant as diffusion progresses. However, for the $\pm 2.0e$ model, exchange events of both species will occur and there will be a

mixing of the ions into the surface. This could possibly be detected experimentally with the use of isotopes. In addition, the $\pm 1.7e$ model predicts a high mobility of the magnesium component of the addimer. This may increase the effective size of the addimer, in terms of a capture cross section for encounters with other species or newly deposited atoms, and qualitatively change the interaction between multiple species on the surface. Thus, while the quantitative changes when going from the $\pm 2.0e$ model to the $\pm 1.7e$ model for addimer diffusion are minor, the qualitative differences may express themselves in more complex environments.

Finally, the TAD results show that the two types of hops and exchanges are indeed the dominant events for both parametrizations, for temperatures of 500 K and below. However, as described above, for both B-G parametrizations, we have seen events that go through the structure illustrated in Fig. 8(b). This structure can be visited via two pathways. First, as mentioned previously, it can be accessed from the exchange minima. In addition, events, though rare, do happen in which the system goes from the ground-state addimer configuration to the structure in Fig. 8(b) and on to a new addimer configuration without visiting the exchange minimum. For the $\pm 2.0e$ model, the barrier for this process is 0.67 eV, while it is 0.61 eV in the $\pm 1.7e$ model. Thus, the rate for this event for the $\pm 1.7e$ model, where it will occur more quickly, is still about four times slower than the dominant path of oxygen hops. At higher temperatures, the difference in the relative probability of these competing pathways will decrease and future work should consider the impact of this diffusion mechanism on film morphology.

III. CONCLUSIONS

We have investigated the diffusion of a MgO addimer on a MgO(100) surface. DFT calculations predict rapid diffusion of the magnesium adion around the oxide ion, which in turn hops along the surface. Magnesium ion exchange with the surface is comparable in energy with a hop, whereas oxide exchange is unfavorable. The exchange process is essentially an interstitialcy mechanism, which is most unusual in most bulk ionic materials, but which appears to be more common at interfaces.[29,30] However, this difference between bulk and surface arises not because the interstitial migration energy itself is high, but is rather due to large Frenkel formation energies in the bulk. At the surface, this formation energy is absent.

A widely used empirical potential model, successfully used previously for many bulk properties, including bulk thermal expansion, defect properties, and high pressure properties, which is based on formal ionic charges of $\pm 2.0e$ fails even qualitatively to reproduce the DFT energy landscape associated with surface diffusion. This striking failure emphasizes that bulk potentials may well be poor for the study of interfaces and, in particular, has led us to consider a partial charge model using Bader atomic charges derived from the DFT calculations. This new potential reproduces the DFT potential energy surface much more successfully than the formal charge model.

In the past, models with partial charges have often been avoided by simulators. They have a number of disadvantages, particularly when defects and impurities are being considered. For example, it is not obvious what partial charges to use in a case such as MgO doped with aluminum ions. However, it is clear from the results presented here that such models can give a better representation of *ab initio* energy surfaces than those using the formal charges expected from simple chemical valence considerations. Also, the Bader algorithm gives a clear, unambiguous method of determining what these reduced charges should be. As such, it is clearly preferable to other methods of obtaining charges, such as Mulliken analysis, which depend on the basis set used.

ACKNOWLEDGMENTS

We would like to thank Jonathan Ball and Robin Grimes for discussion and for providing their Buckingham potential parameters, and Art Voter for hosting each of us at Los Alamos National Laboratory (LANL) and for many interesting discussions. This work was supported by the Robert A. Welch Foundation, grant No. F-160, and the Texas Advanced Computing Center at the University of Texas at Austin. Work at LANL was sponsored by the U.S. DOE Office of Basic Energy Sciences, Division of Materials Sciences and Engineering.

*Corresponding author. Electronic address: henkelman@mail.utexas.edu

[1] A. Atkinson, *Reactive Phase Formation of Interfaces and Diffusion Processes* (Trans. Tech., Zurich, 1994).
[2] M. H. Yang and C. P. Flynn, Phys. Rev. Lett. **73**, 1809 (1994).
[3] E. A. Kotomin, P. W. M. Jacobs, N. E. Christensen, T. Brudevoll, M. M. Kaklja, and A. L. Dopov, Defect Diffus. Forum **143**, 1231 (1997).
[4] S. A. Lytle and V. S. Stubican, J. Am. Ceram. Soc. **65**, 210 (1982).
[5] P. Sajgalik, Z. Panez, and M. Uhrik, J. Mater. Sci. **22**, 4460 (1987).
[6] M. Kubo, Y. Ouru, R. Miura, A. Falimi, A. Stirling, and A. Miyamoto, J. Chem. Phys. **107**, 4416 (1997).
[7] G. Geneste, J. Morillo, and F. Finocchi, Appl. Surf. Sci. **188**, 122 (2002).
[8] G. V. Lewis and C. R. A. Catlow, J. Phys. C **18**, 1149 (1985).
[9] G. Kresse and J. Hafner, Phys. Rev. B **47**, 558 (1993).
[10] G. Kresse and J. Hafner, Phys. Rev. B **49**, 14251 (1994).
[11] G. Kresse and J. Furthmüller, Comput. Mater. Sci. **6**, 16 (1996).
[12] G. Kresse and J. Furthmüller, Phys. Rev. B **54**, 11169 (1996).
[13] J. P. Perdew, in *Electronic Structure of Solids*, edited by P. Ziesche and H. Eschrig (Akademie Verlag, Berlin, 1991).
[14] P. E. Blöchl, Phys. Rev. B **50**, 17953 (1994).

[15] H. J. Monkhorst and J. D. Pack, Phys. Rev. B **13**, 5188 (1976).
[16] G. Henkelman and H. Jónsson, J. Chem. Phys. **113**, 9978 (2000).
[17] G. Henkelman, B. P. Uberuaga, and H. Jónsson, J. Chem. Phys. **113**, 9901 (2000).
[18] G. Henkelman and H. Jónsson, J. Chem. Phys. **111**, 7010 (1999).
[19] B. G. Dick and A. W. Overhauser, Phys. Rev. **112**, 64 (1990).
[20] B. P. Uberuaga, R. Smith, A. R. Cleave, F. Montalenti, G. Henkelman, R. W. Grimes, A. F. Voter, and K. E. Sickafus, Phys. Rev. Lett. **92**, 115505 (2004).
[21] A. F. Voter, F. Montalenti, and T. C. Germann, Annu. Rev. Mater. Res. **32**, 321 (2002).
[22] M. R. Sørensen and A. F. Voter, J. Chem. Phys. **112**, 9599 (2000).
[23] R. Bader, *Atoms in Molecules: A Quantum Theory* (Oxford University Press, New York, 1990).
[24] G. Henkelman, A. Arnaldsson, and H. Jónsson, Comput. Mater. Sci. (to be published).
[25] B. P. Uberuaga, R. Smith, A. R. Cleave, G. Henkelman, R. W. Grimes, A. F. Voter, and K. E. Sickafus, Phys. Rev. B **71**, 104102 (2005).
[26] C. Noguera, F. Finocchi, and J. Goniakowski, J. Phys.: Condens. Matter **16**, S2509 (2004).
[27] J. Ball and R. Grimes (private communication).
[28] J. D. Gale, C. R. A. Catlow, and W. C. Mackrodt, Modell. Simul. Mater. Sci. Eng. **1**, 73 (1992).
[29] D. J. Harris, M. Y. Lavrentiev, J. H. Harding, N. L. Allan, and J. A. Purton, J. Phys.: Condens. Matter **16**, L187 (2004).
[30] D. J. Harris, T. S. Farrow, J. H. Harding, M. Y. Lavrentiev, N. L. Allan, W. Smith, and J. A. Purton, Phys. Chem. Chem. Phys. **7**, 1839 (2005).